第41卷第10期 中国科学技术大学学报 Vol. 41, No. 10
2011年10月 JOURNAL OF UNIVERSITY OF SCIENCE AND TECHNOLOGY OF CHINA Oct. 2011

Article ID: 0253-2778(2011)10-0855-07

Synthesis of decoupage-like carbon sheets and their adsorption properties

ZHENG Xiandong[1], ZHU Yongchun[1], JU Zhicheng[2], LI Qianwen[1], QIAN Yitai[1]

(1. *Hefei National Laboratory for Physical Science at Microscale and Department of Chemistry, University of Science and Technology of China, Hefei* 230026, *China*;
2. *Key Laboratory of Colloid and Interface Chemistry (Shandong University), Ministry of Education, and School of Chemistry and Chemical Engineering, Shandong University, Jinan* 250100, *China*)

Abstract: Decoupage-like carbon sheets (DLCSs) were obtained on a large scale by pyrolysis of tetrachloroethylene and ferrocene in an autoclave at 600 ℃ for 10 h. The scanning electron microscopy (SEM) images show that the thickness and the width of DLCSs are about 20～40 nm, 100～200 nm, respectively. The nitrogen adsorption/desorption isotherm experiments reveal that the Brunauer-Emmett-Teller (BET) specific surface area of the product is 1 209 m^2/g and the pore-size distribution is concentrated in the range of 0.58～1.2 nm. A series of comparative experimental results demonstrate that the most favorable temperature, amount of ferrocene and reaction time are 600 ℃, 0.093 g and 10 h for synthesis of DLCSs. By adjusting reaction parameters, hollow carbon spheres and carbon sheets can also be selectively prepared using one-pot reactions. A possible formation mechanism for the DLCSs was proposed based on the diffusion-limited aggregation(DLA) model. The adsorption behavior of DLCSs were evaluated by the removal of phenol and Rhodamine B (RB), which can remove about 82% of phenol and 48% of RB without any other additives. A possible reason for this phenomenon was also discussed.

Key words: carbon nanomaterials; scanning electron microscopy (SEM); Brunauer-Emmett-Teller (BET); solvothermal pyrolysis

CLC number: O611.4 **Document code**: A doi: 10.3969/j.issn.0253-2778.2011.10.002

剪纸状碳的合成及其吸附性能

郑贤东[1], 朱永春[1], 鞠治成[2], 李倩文[1], 钱逸泰[1]

(1. 中国科学技术大学化学与材料科学学院, 化学系, 安徽合肥 230026; 2. 山东大学化学与材料科学学院, 化学系, 山东济南 250100)

摘要: 以二茂铁和四氯乙烯作为反应物, 采用热解法在600 ℃反应10 h得到一种高产率的剪纸状的碳片. 扫

Received: 2011-04-15; **Revised**: 2011-05-26

Foundation item: Supported by National Natural Science Foundation of China (91022033) and the National Key Basic Research (973) Program of China (2011CB935900).

Biography: ZHENG Xiandong, male, born in 1985, master. Research field: synthesis of carbon nanomaterials. E-mail: xiaodong@mail.ustc.edu.cn

Corresponding author: ZHU Yongchun, Prof. E-mail: ychzhu@ustc.edu.cn

描电镜的结果表明,剪纸状碳材料的厚度为 20～40 nm,宽度为 100～200 nm.通过氮气吸附-脱附等温曲线计算出产物的比表面积高达1 209 m^2/g,孔径分布在 0.58～1.2 nm 之间.一系列对比实验表明,合成剪纸状碳材料的最佳条件为:0.093 g 二茂铁,反应温度为 600 ℃,反应时间为 10 h.通过调整二茂铁与四氯乙烯的比例,可控制产物的形貌从剪纸状转化为空心球.剪纸状碳对于苯酚的吸附性能(82%)要远高于对罗丹明 B 的吸附性能(48%),并对其给出了可能的解释.

关键词:碳纳米材料;扫描电子显微镜;比表面积;热解

0 Introduction

Recently, there have been numerous reports about the formation of two-dimensional (2-D) carbon nanostructures owning to their remarkable surface area, smooth surface morphologies and thin edges, flexibility and elasticity, high thermal and chemical stability, and lightness[1-2]. The carbon nanostructures with 2-D structures may have potential applications, such as promising candidates for adsorbent[3], hydrogen storage materials[4], catalyst supports[5], sensors[6] or electrode materials for lithium-ion batteries[7].

Up to now, various approaches have been carried out to prepare 2-D carbon nanostructures. For example, carbon sheets with a thickness of 300～500 nm composed of two layer planes were synthesized at 600 ℃ by solvothermal process[8]. Well-separated carbon sheets on a variety of substrates were synthesized by a radio frequency plasma enhanced chemical vapor deposition method[9] and by a hot filament chemical vapor deposition method[10-11]. The flower-like carbon nanosheet aggregations with 2～4 μm in diameter were prepared by reacting ferrocene and carbon disulfide at 800 ℃, in which the composed carbon nanosheets were 5.1 ～ 8.0 nm in thickness[12]. Leaf-like carbon sheets using Cu ribbons as substrates were obtained by ferrocene and methylene dichloride in 300 ～ 600 ℃, and the thickness of the sheets could be controlled from 50 to 200 nm by adjusting the experimental parameters[13].

Herein, we report the one-pot synthesis of DLCSs with a flake in the middle and some ribbon around the flake by an easy pyrolysis process at 600 ℃. The thickness of DLCSs is about 20～40 nm. It is worth noting that the value of BET specific surface area is 1 209 m^2/g and the pore size is concentrated in the range of 0.58 ～ 1.2 nm. Besides 2-D DLCSs, hollow carbon spheres and carbon sheets could also be selectively prepared by adjusting reaction parameters. Moreover, adsorption behavior of DLCSs have also been studied.

1 Experimental

1.1 Preparation of DLCSs

All the chemical reagents were of analytical purity and purchased from Shanghai Chemical Reagents Company. In a typical procedure, Tetrachloroethylene (2 mL, 97.0%) and ferrocene powders (0.093 g, 99.5%) were mixed in an autoclave of 20 mL capacity. The autoclave was sealed and heated in an electric stove with a heating ramp rate of 10 ℃/min and maintained at 600 ℃ for 10 h. Afterwards, the autoclave was cooled to room temperature naturally. A dark powder was collected and washed with hydrochloric acid, distilled water and ethanol. The final product was dried in vacuum at 60 ℃ for 10 h.

1.2 Adsorption experiment

20 mL of phenol solution (100 $mg \cdot L^{-1}$) was mixed with 30 mg of DLCSs product in the volume of 50 mL glass bottle, and the mixture was maintained for 120 min while stirring. Then it was filtered with filter paper and residual phenol concentration in the filtrate was determined. The standard absorption of phenol at 270 nm was chosen for monitoring the adsorption process. For comparison, Rhodamine B (RB) was also used as an adsorbate repeating the former experiment. The

standard absorption of RB at 553 nm was chosen for monitoring the adsorption process.

1.3 Characterization

The final products were characterized by powder X-ray diffraction (XRD) (Philips X'pert diffractometer with Cu $K\alpha_1$ radiation(λ=1.541 78 Å)), scanning electron microscopy (SEM, HITACHIX-650 and JEOLJSM-6700F), high-resolution transmission electron microscopy (HRTEM, JEOL 2010 using an accelerating voltage of 200 kV), A TU-1901 UV/Vis spectrometer, Raman spectroscopy (RS, Spex 1 403 Raman spectrometer with an argon ion laser at an excitation wavelength of 514.5 nm) and the Brunauer-Emmett-Teller (BET, ASAP 2020).

2 Results and discussion

2.1 Structure and morphology

The XRD pattern of the products is shown in Fig. 1(a). It is observed that the broad diffraction peak (~23.8°) with low diffraction intensity could be indexed to the (0 0 2) diffractions of turbostratic, and polyaromatic carbon. The position of the (002) peak shifts from 26.48° for graphite to 23.8°, which corresponds to an increase in the spacing between the sp^2-carbon layers from 0.337 nm for graphite to 0.372 nm for the product. The result is similar to the observation of other related carbon materials[14-15]. In addition, the broad peak around 43~45° could be attributed to (1 0) diffractions of carbon. The broad peaks in the XRD patterns indicate the existence of highly disordered structures in the products.

The typical Raman spectrum of the product in Fig. 1(b) shows that there are two strong peaks at 1 340 cm^{-1} and 1 597 cm^{-1}, respectively. The peak at 1 340 cm^{-1}, named D-band, corresponds to the vibration of carbon atoms with dangling bonds for the in-plane terminations of disordered graphite. The peak at 1 597 cm^{-1}, named G-band, could be assigned to an E2g vibration mode of graphite and is related to the vibration of sp^2-bonded carbon atoms in a 2-D hexagonal lattice. These results prove that the existence of carbon materials in the as-obtained products. It is worth mentioning that, the intensity of the D-band higher than that of the G-band is due to the defects and partially disordered crystal structure of the product, suggesting that the products have lots of defects, in accordance with the results of XRD pattern.

The morphologies of the as-prepared samples were observed by SEM. A typical low-magnification SEM image of the sample is shown in Fig. 2(a). It can be seen that DLCSs account for the majority of the product, and few irregular particles are observed. Fig. 2(b) and inset of Fig. 2(b) show the high-magnification SEM image of sample, which indicates that the typical product is composed of a flake in the middle with some ribbons around it. The thickness of the flake is about 20~40 nm, and the width of the ribbon is about 100~200 nm. HRTEM and SAED pattern

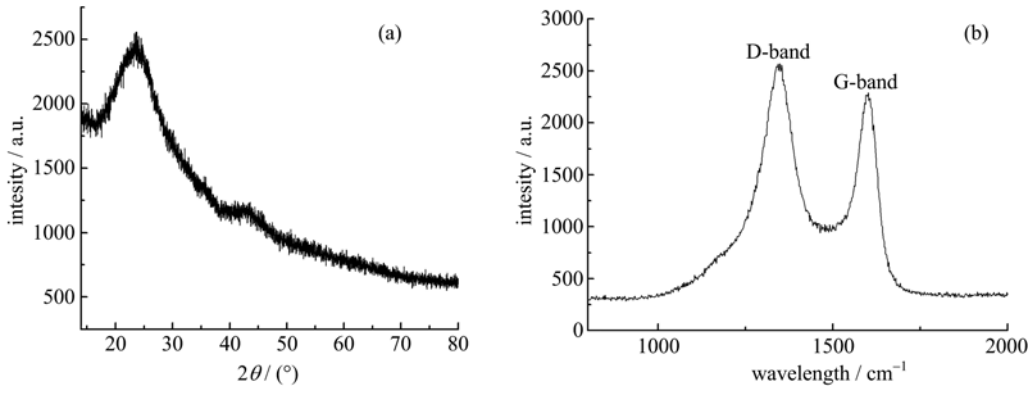

Fig. 1 (a) Typical XRD patterns of the product, and (b) Raman spectrum of the product at room temperature

of the product in Fig. 2(c) indicate that these DLCSs are highly disordered structures, in accordance with the results of XRD and Raman spectrum. Inset of Fig. 2(c) presents the SAED pattern of the products, in which relatively weak circles can be indexed to (0 0 2) and (1 0) planes of carbon.

2.2 Influencing factors

A series of relevant experiment have been carried out to investigate the effect of reaction conditions on the formation of DLCSs. It is found that temperature, amount of ferrocene and reaction time are important factors influencing the yields of DLCSs. When the temperature was lower than 400 ℃, there were no DLCSs in the product. If the temperature was raised to 500 ℃, the main products were carbon nanosheets and only a small quantity of DLCSs, just as shown in Fig. 3(a). When the temperature was increased to 600 ℃, the sample was almost entirely DLCSs (as shown in Fig. 2(a)). Even if the temperature was elevated to 700 ℃, a large amount of DLCSs could also be observed in the product. Those experiments show that the morphologies of the product vary from carbon nanosheets to DLCSs by adjusting the temperature. Fig. 3 (b) ~ (d) show the morphologies of the product synthesized at 600 ℃ for 10 h using different amounts of ferrocene. When the amount of ferrocene was 0.050 g, a lot of carbon nanosheets and small amounts of

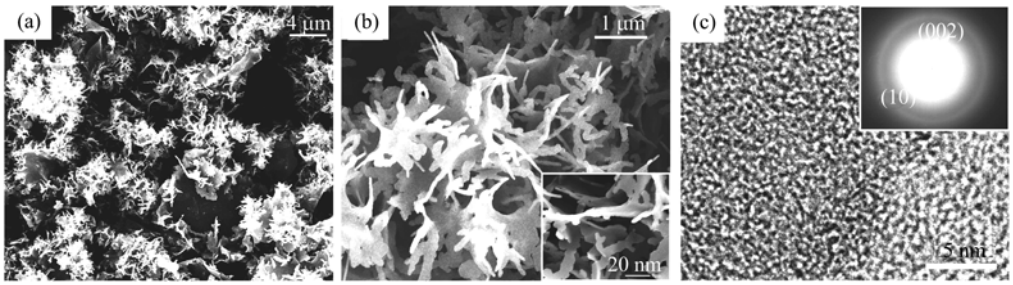

(a) low magnification (b) high magnification (c) HRTEM and SAED of the products

Fig. 2 FESEM images of the products

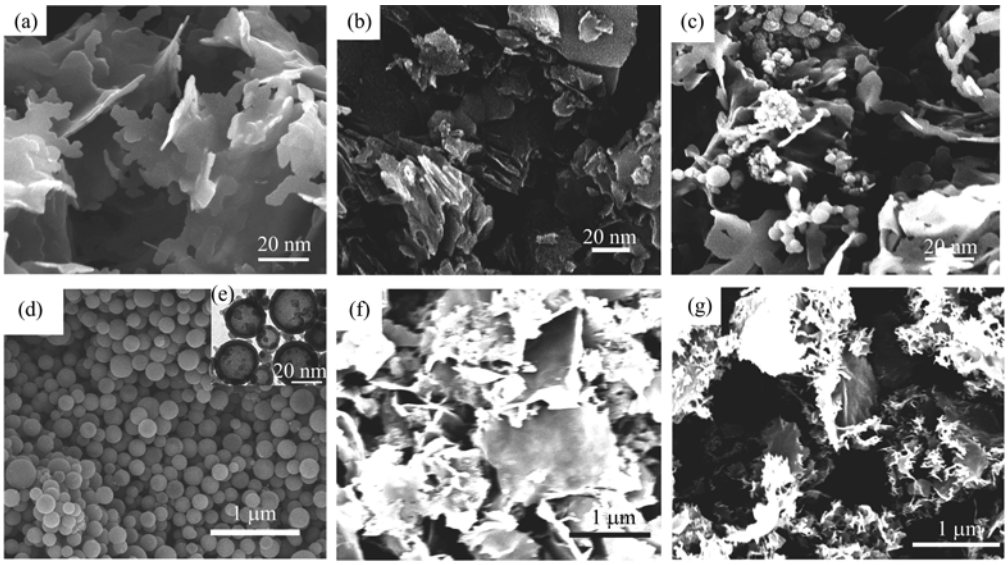

(a) SEM of products at 500 ℃ for 10 h, (b)~(d) SEM of the products when the amount of the ferrocene is 0.005, 0.186, 0.279 g, respectively, (e) TEM of the products when the amount of the ferrocene is 0.279 g (inserted in Fig. 3(d)), (f)~(g) SEM images of the products obtained at 600 ℃ for 4 h and 8 h, respectively

Fig. 3 SEM images of the products from comparative experiment

irregular particles could be obtained (Fig. 3(b)). When increasing the amount of the ferrocene to 0.093 g, it was observed that almost all the products are DLCSs (Fig. 2 (a)). When the amount of the ferrocene increased to 0.186 g, the product was made up of some carbon nanospheres besides DLCSs (Fig. 3(c)). When the amount of ferrocene was 0.279 g, the product was dominated by carbon nanospheres with diameters about 100 ~ 200 nm (Fig. 3 (d)). Interestingly, the spheres in the Fig. 3(d) was mostly hollow (Fig. 3(e) inserted in Fig. 3(d)) which is similar to the previous work[16]. All the above experiments indicate that the transformation from DLCSs to hollow carbon nanospheres could be achieved by adjusting the amount of ferrocene. The SEM images of the corresponding sample obtained at different reaction times are shown in Fig. 3(f)~(g). After 4 h, the main products were irregular flakes (Fig. 3(f)). As the reaction time increased to 8 h, many ribbons appeared at the edge of the flake, which can be clearly observed in Fig. 3(g). If the reaction time reached 10 h, almost all of the products were DLCSs (Fig. 2 (a)). Therefore, the most favorable temperature, amount of ferrocene and reaction time were 600 ℃, 0.093 g and 10 h for synthesis of DLCSs.

Based on the above experimental results, we try to explain a possible mechanism on the basis of the diffusion-limited aggregation(DLA) model[17]. With the temperature rising, at first, $Fe(cp)_2$ and C_2Cl_4 are decomposed, C and Fe atoms are form[13,18] which undergo a "random walk" due to Brownian motion, and these C atoms would aggregate to form fractal (Fig. 3 (f)) due to their inherently anisotropic growth and asymmetric condensation in stainless steel autoclaves[10]. In the second step, residual carbon atoms start to extend along one direction under lower vapor pressure for minimizing the energy of the reaction[19], as seen in Fig. 3(g). In the end, DLCSs are formed. In addition, the ring structures of the ferrocene may contribute to the formation of two dimensional structures. When Fe atoms exceed threshold by increasing the amount of $Fe(cp)_2$, these Fe atoms would aggregate to form clusters[18], which act as a template and catalyst for the initial carbon hollow sphere formation. As the reaction proceeds, the inner Fe core is etched away by Cl atoms to form the carbon hollow sphere (Fig. 3(d),(e)).

2.3 The N_2 adsorption-desorption isotherm and pore diameter distribution

The BET specific surface area and pore size distribution of DLCSs are determined from nitrogen adsorption/desorption isotherm (Fig. 4 (a)), which exhibits type IV characteristics. The curve displays a hysteresis loop at a relative pressure (P/P_0) being 0.4 ~ 1.0, which means that the resultant product may possess framework structures[13]. Meanwhile, the large volume

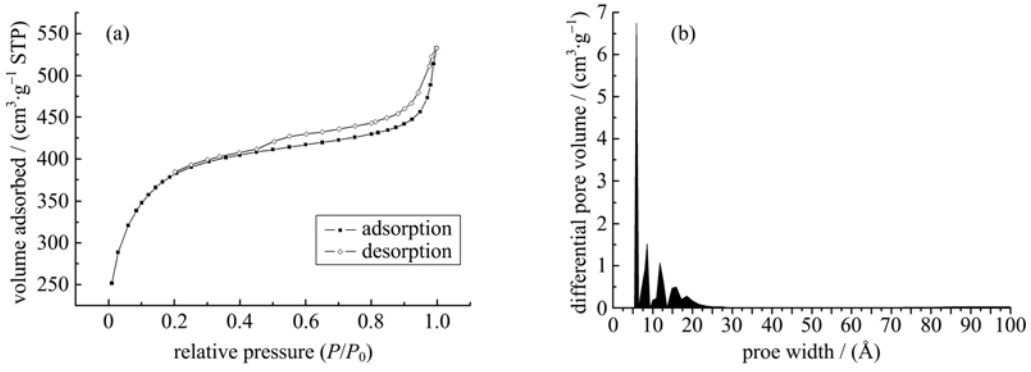

Fig. 4 (a) Typical N_2 adsorption-desorption isotherm of DLCSs obtained at 600 ℃, and (b) pore size distribution of DLCSs obtained by DFT method

adsorbed at the lower P/P_0 being 0～0.2 suggests the presence of lots of microporosity[20]. The loop does not close below the relative pressure $P/P_0 = 0.42$. It is possible to the deformation of a nonrigid porous structure or to the irreversible adsorption of molecules in extremely small micropores. The BET surface area of DLCSs calculated from the results of nitrogen adsorption reach about 1 209 m^2/g, which is much higher than that of leaf-like carbon sheets of 398 m^2/g[13]. The total pore volume and micropore pore volume are 0.74 cm^3/g and 0.51 cm^3/g, respectively. At the same time, pore size distribution of the DLCSs is analyzed based on the density functional theory (DFT) method. As seen in Fig. 4(b), the pore size of the DLCSs is concentrated in the range of 0.58 ～1.2 nm, in which more than 60% of the pore size is 0.58 nm.

2.4 Adsorption behavior

Carbon materials are commonly used as adsorbent for the removal of organic waste from water by adsorption at relatively low temperature[21-22]. Herein, using the prepared DLCSs as adsorbent, we investigated their application in water treatment.

Phenol was selected for the adsorption experiment due to its presence in the wastewaters of some industries (such as leather, jute, textile and food industries)[23]. To eliminate it and develop low-cost adsorbents has become more and more important. UV/Vis absorption spectroscopy[24] was applied to record the adsorption behavior of the solution before and after treatment by DLCSs (Fig. 5). The standard absorption of phenol at 270 nm was chosen for monitoring the adsorption process. The result demonstrates that the as-prepared DLCSs can remove most of the phenol at room temperature as shown by the UV/Vis absorption spectra in Fig. 5 (a), with a removal capacity of 82% of phenol without any other additives, which showed a much better removal capacity than previous reports on commercial activated carbon (33.3%)[25]. For comparison, we also used Rhodamine B (RB) as an adsorbate repeating the former experiment. The standard absorption of RB at 553 nm was chosen for monitoring the adsorption process. It is found that the removal capacity of RB was 48% (seen in Fig. 5(b)). It is obvious that the amount of RB adsorbed onto the DLCs is much less than the amount of phenol onto the DLCs under the same conditions. Since the molecular size of RB (L: 1.8 nm; B: 0.7 nm)[21] is larger than the dominant pore size of the DLCSs (0.58 ～ 1.2 m), Therefore, after the pore has adsorbed RB molecules at the opening, it will hinder the subsequent entrance of RB molecules and cannot diffuse into small micropores. However, phenol with smaller molecular size was able to diffuse more easily into the pores of the DLCSs than RB.

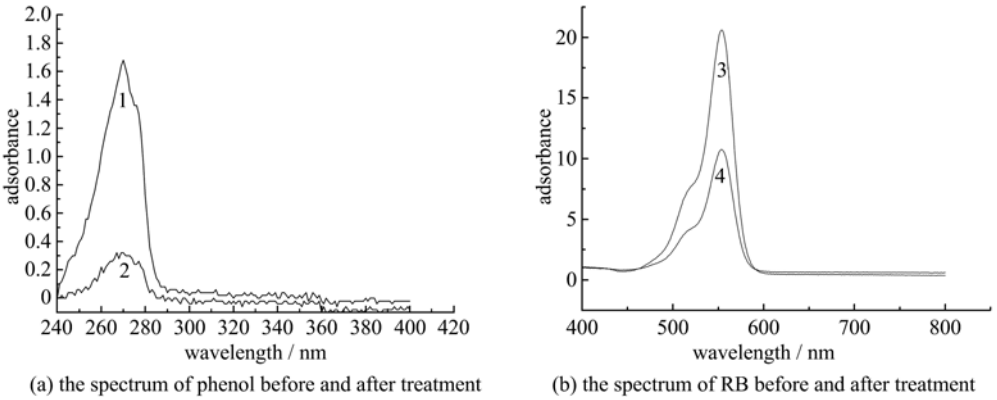

(a) the spectrum of phenol before and after treatment (b) the spectrum of RB before and after treatment

Fig. 5 UV/Vis absorption spectra of phenol and RB

3 Conclusion

In summary, DLCSs were synthesized by mixing Tetrachloroethylene and ferrocene at 600 ℃. The specific surface area of DLCSs reaches as far as 1 209 m^2/g. Temperature, amount of the ferrocene and reaction time are found to play important roles in the formation of DLCSs. The adsorption behavior of DLCSs were evaluated by the removal of phenol and RB, which can remove about 82% of phenol and 48% of RB without any other additives. This may be attributed to the different molecular sizes of phenol and RB. Therefore, they might have potential applications in many areas, such as adsorbents, catalyst supports, electrode materials, and energy-storage media.

References

[1] Chung D D L. Review graphite[J]. J Mater Sci, 2002, 37: 1 475-1 489.

[2] Manning T J, Mitchell M, Stach J, et al. Synthesis of exfoliated graphite from fluorinated graphite using an atmospheric-pressure argon plasma[J]. Carbon, 1999, 37: 1 159-1 164.

[3] Yang Kun, Wu Wenhao, Jing Qingfeng, et al. Aqueous adsorption of aniline, phenol, and their substitutes by multi-walled carbon nanotubes [J]. Environ Sci Technol, 2008, 42: 7 931-7 936.

[4] Gao Fen, Zhao Dongli, Li Yan, et al. Preparation and hydrogen storage of activated rayon-based carbon fibers with high specific surface area [J]. J Phys Chem Solids, 2010, 71: 444-447.

[5] Qin Yuanhang, Yang Houhua, Zhang Xinsheng, et al. Electrophoretic deposition of network-like carbon nanofibers as a palladium catalyst support for ethanol oxidation in alkaline media [J]. Carbon, 2010, 48: 3 323-3 329.

[6] Guo Shaojun, Wen Dan, Zhai Yueming, et al. Platinum nanoparticle ensemble-on-graphene hybrid nanosheet: One-pot, rapid synthesis, and used as new electrode material for electrochemical sensing[J]. Acs Nano, 2010, 4: 3 959-3 968.

[7] Mei Tao, Li Ting, Bi Huiyun, et al. Synthesis and electrical capacitance of carbon nanoplates[J]. Eur J Inorg Chem, 2010, 27: 4 314-4 320.

[8] Xiao Yong, Liu Yingliang, Cheng Liqiang, et al. Flower-like carbon materials prepared via a simple solvothermal route[J]. Carbon, 2006, 44: 1 581-1 611.

[9] Zhu M Y, Wang J J, Holloway B C, et al. A mechanism for carbon nanosheet formation [J]. Carbon, 2007, 45: 2 229-2 234.

[10] Shang N G, Au F C K, Meng X M, et al. Uniform carbon nanoflake films and their field emissions[J]. Chem Phys Lett, 2002, 358: 187-191.

[11] Kurt R, Bonard J M, Karimi A. Morphology and field emission properties of nano-structured nitrogenated carbon films produced by plasma enhanced hot filament CVD[J]. Carbon, 2001, 39: 1 723-1 730.

[12] Shen Jianmin, Feng Yitao. Formation of flower-like carbon nanosheet aggregations and their electrochemical application[J]. J Phys Chem C, 2008, 112: 13 114-13 120.

[13] Ju Zhicheng, Wang Tingting, Wang Liancheng, et al. A simple pyrolysis route to synthesize leaf-like carbon sheets[J]. Carbon, 2010, 48: 3 420-3 426.

[14] Hu Gang, Cheng Mojie, Ma Ding, et al. Synthesis of carbon nanotube bundles with mesoporous structure by a self-assembly solvothermal route[J]. Chem Mater, 2003, 15: 1 470-1 473.

[15] Kercher A K, Nagle D C. Microstructural evolution during charcoal carbonization by X-ray diffraction analysis[J]. Carbon, 2003, 41: 15-27.

[16] Xu Liqiang, Zhang Wanqun, Yang Qing, et al. A novel route to hollow and solid carbon spheres [J]. Carbon, 2005, 43: 1 090-1 092.

[17] Huang L J, Lau W M. Multifractal analysis of two-dimensional carbon clusters [J]. J Phys: Condens Matter, 1993, 5: 7 087-7 094.

[18] Xiong Yujie, Xie Yi, Li Xiaoxu, et al. Production of novel amorphous carbon nanostructures from ferrocene in low-temperature solution[J]. Carbon, 2004, 42: 1 447-1 453.

[19] Ma Xiying, Yuan Baohe. Fabrication of carbon nanoflowers by plasma-enhanced chemical vapor deposition[J]. Appl Surf Sci, 2009, 255: 7 846-7 850.

[20] Lim W C, Srinivasakannan C, Balasubramanian N. Activation of palm shells by phosphoric acid impregnation for high yielding activated carbon[J]. J Anal Appl Pyrol, 2010, 88: 181-186.

[21] Guo Yupeng, Zhao Jingzhe, Zhang Hui, et al. Use of rice husk-based porous carbon for adsorption of Rhodamine B from aqueous solutions [J]. Dyes

(下转第 866 页)